P41B-3424

# Inversion of occultation observation of a dusty atmosphere using hypergeometric functions.


B. Hubert[(1)] , J.-C. Gérard[(1)] , L. Gkouvelis[(1)], B. Ritter [(1&2)], A. Piccialli[(3)] and A.-C. Vandaele[(3)] .

1. Space sciences, Technologies and Astrophysics Research Institute, University of Liège, Liège, Belgium
2. Royal Observatory of Belgium
3. Royal Belgian Institute for Space Aeronomy

Contact: B.Hubert@ulg.ac.be



## Summary

Occultation of solar radiation by a planetary atmosphere is a very accurate method to obtain high signal vs noise spectral measurement of the properties of the atmospheric gas, not only owing to the overwhelmingly large photon flux from our host star, but also because the method is nearly not dependent on instrument calibration. On the other hand, the method can only be applied near the terminator. Using occultation techniques in other regions of the atmosphere can nevertheless be done using stars as a radiation source, but the instrument then has to be more sensitive to cope with the severely reduced photon flux. The method nevertheless remains independent on the absolute calibration of the instrument.

Occultation observation directly provides the optical thickness (or the extinction coefficient) of the absorbing and scattering constituents when multiple scattering can be safely neglected. Under those conditions, the measurement gives the line-of-sight integrated density of the absorbing and scattering constituents, and simultaneous measurements at several wavelength are then needed to discriminate between the effects of the several species. Retrieval of the vertical density profile of the different constituents requires an inversion method, basically an inverse Abel transform when a spherical (or cylindrical) symmetry assumption can be made.

Efficient inverse Abel transform methods rely on least squares fit techniques taking advantage of easy-to-compute analytical indefinite integrals constructed from the Abel transform integral operator. In the case of a dusty atmosphere, the contribution of dusts to the extinction depends on the properties of the dust grains controlling their scattering cross section, which is generally represented using the so-called alpha parameter appearing as an exponent of the wavelength in the expression of the cross section. As the properties of the dusts vary with altitude, so does the alpha parameter, which severely complicates the computation of the indefinite integrals needed for the inverse Abel transform fitting. We propose a method that allows to express those indefinite integrals using Gauss's hypergeometric 2F1 function, which can be applied to the observation of the Earth as well as of planet Mars, as it is done by the ESA EXOMARS-NOMAD instrument.


## Atmosphere remote sensing: Abel transform

Remote sensing instruments used to study the emissions of the atmosphere of celestial objects (planets and comets) produce line-of-sight integrated quantities. For example, observations of the radiations directly emitted by the atmosphere integrate the volume emission rate (VER) along the instrument line of sight (l.o.s.), in the optically thin case. For occultation observations, the observed radiation coming from the sun (or from a star) is attenuated by the slant gas column integrating the atmospheric gas density along the l.o.s. When the integrated quantity, either the VER or an atmospheric constituent density, can be assumed to have a spherical symmetry, this l.o.s. integration is called the Abel transform of this quantity.

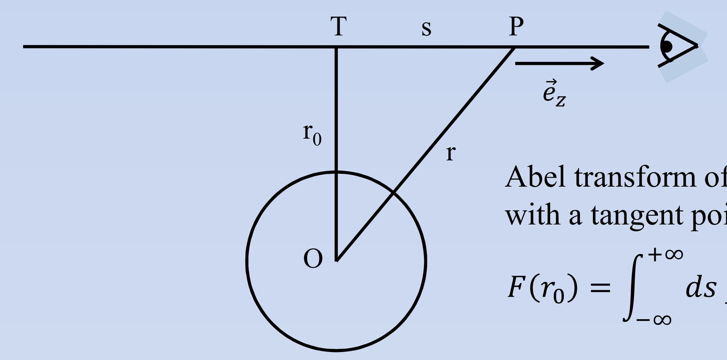


Abel transform of function f(r) along a line of sight with a tangent point located at the radial distance $r_0$:

$$F(r_0) = \int_{-\infty}^{+\infty} ds\, f(s) = 2\int_{r_0}^{+\infty} dr\, \frac{r}{\sqrt{r^2-r_0^2}} f(r) \quad (1)$$

Function f(r) represents the VER or a gas density and $F(r_0)$ its Abel transform as a function of $r_0$ the tangent radius of the l.o.s.. The gas numeric density profile can have several functional expressions. In planetary atmospheres, it is often represented by an exponential profile (2) or by a Chapman profile (3).

$$n(r) = n_0\, e^{-\frac{r-r_0}{H}} \quad with\ H = \frac{kT}{mg} \quad (2)$$

$$n(r) = n_0 \exp\left(1 - \frac{r-r_0}{H} - \frac{1}{\mu}\exp\left(-\frac{r-r_0}{H}\right)\right) \quad (3)$$

Retrieving the local quantity f(r) from the knowledge of its Abel transform $F(r_0)$ is, in principle, feasible using the analytical inversion formula:

$$f(r) = \frac{-1}{\pi}\int_r^{\infty} dr_0\, \frac{1}{\sqrt{r_0^2-r^2}}\frac{dF(r_0)}{dr_0} \quad (4)$$

Applying this formula to real observation is however difficult because the derivative of the observation can be dominated by the noise, the profile needs to be known up to high altitude, and a sufficiently high sampling is needed to reliably carry the integration. One generally resorts to least squares fitting methods to overcome these drawbacks.

## Inverse Abel transform using least squares fitting

The general idea of numerical Abel transform inversion is to f(r) using locally defined functions, such as a set of line segments (i.e. a piecewise linear function) of which the Abel transform can be computed, and determine the parameters of each piece by fitting the Abel transform of the piecewise-defined vertical profile on the observation, so f(r) is immediately known.

The first method that comes to mind is to represent f(r) with line segments. This choice clearly illustrates the principle of the method: a piecewise linear function can be represented by the linear combination of triangular functions $t_k(r)$ defined on overlapping intervals. The Abel transform $T_k(r_0)$ of each triangle $t_k(r)$ can be computed, and a linear combination of the $T_k$'s can be fitted over the observed $F(r_0)$ denoting $\chi_\Omega(r)$ the function that is 1 for $r \in \Omega$, and 0 otherwise:

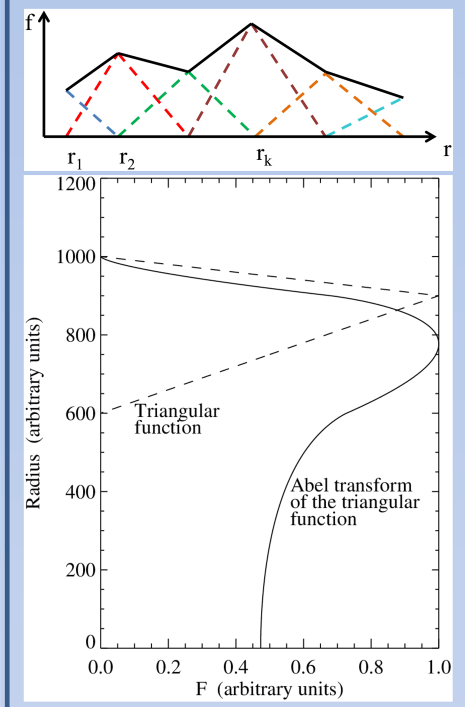


$$t_k(r) = \frac{r-r_{k-1}}{r_k-r_{k-1}}\chi_{]r_{k-1},r_k[}(r) + \frac{r_{k+1}-r}{r_{k+1}-r_k}\chi_{]r_k,r_{k+1}[}(r)$$

$$f(r) = \sum_k a_k t_k(r) \qquad F(r_0) = \sum_k a_k T_k(r_0)$$

$$T_k(r_0) = 2\int_{r_0}^{+\infty} dr\, \frac{r}{\sqrt{r^2-r_0^2}} t_k(r) = 2\int_{r_{k-1}}^{r_k+1} dr\, \frac{r}{\sqrt{r^2-r_0^2}} t_k(r) \quad (5)$$

Computation the Abel transform of individual triangular elements requires computing indefinite integrals constructed from the Abel transform. This can be easily done when the elements only contain powers of r. One can however use triangular elements that differ from the linear triangles of equation (5), to account for the needs of a specific observation.

In the case of occultation studies, the observation provides the l.o.s. integrated gas density in an indirect manner. A scan measuring the brightness (or intensity) I for a set of different values of r0 at several wavelength λ allows for the estimate of the intensity ratio

$$\frac{I(r_0,\lambda)}{I_{top}(\lambda)} = \exp\left(-\sum_{j=1}^{n_{abs}}\sigma_j(\lambda)\mathcal{N}_j(r_0) - \tau_{dust}(r_0,\lambda)\right)$$

$$\mathcal{N}_j(r_0) = 2\int_{r_0}^{\infty} dr\, \frac{r}{\sqrt{r^2-r_0^2}} n_j(r)$$

$$\tau_{dust}(r_0,\lambda) = 2\int_{r_0}^{\infty} dr\, \frac{r}{\sqrt{r^2-r_0^2}} k_{ext}(r,\lambda) \quad (6)$$

$$k_{ext}(r,\lambda) = k_{ext0}(r)\left(\frac{\lambda_0}{\lambda}\right)^{\alpha(r)}$$

$$n_j(r) \approx \sum_k a_{j,k}\, t_k(r) \qquad \mathcal{N}_j(r) \approx \sum_k a_{j,k}\, T_k(r)$$

$$k_{ext_0} \approx \sum_k a_k^d\, t_k(r) \qquad \alpha(r) \approx \sum_k b_k^d\, u_k(r)$$

$$K_k = 2\int_{r_{k-1}}^{r_{k+1}} dr\, \frac{r}{\sqrt{r^2-r_0^2}} t_k(r)\left(\frac{\lambda_0}{\lambda}\right)^{\alpha(r)}$$

Where $I_{top}$ denotes the unattenuated intensity of light source at the top of the atmosphere (i.e. for very large $r_0$), $n_{abs}$ is the number of absorbing species in the atmosphere (such as $O_3$ in the near UV), $\sigma_j$ is the absorption cross section of the $j^{th}$ specie, $\mathcal{N}_j$ is the slant column density resulting from the l.o.s. integration of the number density $n_j$ (that will be approximated with a piecewise linear function). The optical thickness of dusts, $\tau_{dust}$ is obtained by l.o.s. integration of the dust extinction coefficient $k_{ext}$, given by the extinction coefficient $k_{ext0}$ (with piecewise linear approximation) at reference wavelength $\lambda_0$ multiplied by the ratio $\lambda_0/\lambda$ elevated to power α(r) (O'Niel and Royer, 1993). The α parameter will be piecewise-represented using appropriate functions $u_k(r)$ to be introduced later as to make the computation of $K_k(r_0)$ manageable.

Assuming first that the $b_k^d$ are known and that the Abel transform of all the triangular elements is know, the inverse Abel transform problem reduces to a linear system solving the least squares fitting of the data, generally with a Tikhonov regularization weighted by a parameter γ. Packing the $a_{j,k}$ and the $a_k^d$ in one single array $\vec a$ (components $a_k$) and denoting the Abel transform of the corresponding triangular element (either $T_k$ or $K_k$) as $F_k$, finding the inverse Abel transform reduces to alinear least squares fitting. We apply a regularization matrix that computes the second derivative of the fitted $a_k$'s, as if they were a function of the radial distance: this penalizes noisy variations (Hubert et al., 2016). (Observations $G_j$ pack the $\ln(I(r_{0,j},\lambda_j)/I_{top}(\lambda_j))$ in one single array.)

$$\chi^2 = \sum_{j=1}^{J}\left(G_j - \sum_k a_k F_k(r_{0,j})\right)^2 w_j \qquad H_{ik} = \sum_{j=1}^{J} F_i(r_{0,j})\, F_k(r_{0,j})\, w_j = (\mathbf{F V_G^{-1} F^+})_{ik}$$

$$\boldsymbol{H}\vec a = \vec b \qquad b_i = \sum_{j=1}^{J} G_j\, F(r_{0,j})\, w_j \qquad F_{ji} = F_i(r_{0,j}) \quad (7)$$

$$(\boldsymbol{H} + \gamma\boldsymbol{Q})\,\vec a = \vec b$$

$$\gamma = c\,\frac{tr(\boldsymbol{H})}{tr(\boldsymbol{Q})}$$

Regularization matrix (Hubert et al., 2016)

$\mathbf{V_G}$ : variance matrix of the observation $\{G_j\}$

## Abel transform of triangular elements for dust

Computing the Abel transform $K_k$ of equation (6) requires to suitably chose the elementary functions $u_k(r)$. Using the $t_k$ of equation (5) to build the piecewise approximation of the α exponent parameter leads to Abel transforms of exponential-polynomial functions, which is complicated and computationally costy. Using constant α value over each $[r_k, r_{k+1}[$ interval is the easiest $u_k$ choice. We also build triangular elements linear with respect to the logarithm of the radial distance. Choosing a reference radial distance $r^*$ (typically, the planet radius), we write

$$u_k(r) = \frac{\ln\left(\frac{r}{r^*}\right) - \ln\left(\frac{r_{k-1}}{r^*}\right)}{\ln\left(\frac{r_k}{r^*}\right) - \ln\left(\frac{r_{k-1}}{r^*}\right)}\chi_{]r_{k-1},r_k[}(r) + \frac{\ln\left(\frac{r_{k+1}}{r^*}\right) - \ln\left(\frac{r}{r^*}\right)}{\ln\left(\frac{r_{k+1}}{r^*}\right) - \ln\left(\frac{r_k}{r^*}\right)}\chi_{]r_k,r_{k+1}[}(r) \quad (7)$$

$$t_k(r)\left(\frac{\lambda_0}{\lambda}\right)^{\alpha(r)} = t_k(r)\left(\frac{\lambda_0}{\lambda}\right)^{b_{k-1}^d u_{k-1}(r) + b_k^d u_k(r) + b_{k+1}^d u_{k+1}(r)}$$

Accounting for the non-zero support of $t_k$ , so that we can rewrite the dust optical thickness:

$$\tau_{dust} = 2\sum_k \frac{a_k^d}{r_k - r_{k-1}}\left(\frac{\lambda_0}{\lambda}\right)^{\frac{b_{k-1}^d\ln\left(\frac{r_k}{r^*}\right) - b_k^d\ln\left(\frac{r_{k-1}}{r^*}\right)}{\ln\left(\frac{r_k}{r^*}\right) - \ln\left(\frac{r_{k-1}}{r^*}\right)}}\int_{r_{k-1}^*}^{r_k^*} dr\, \frac{r\,(r - r_{k-1})}{\sqrt{r^2-r_0^2}}\left(\frac{r}{r^*}\right)^{\ln\left(\frac{\lambda_0}{\lambda}\right)\frac{-b_{k-1}^d + b_k^d}{\ln\left(\frac{r_k}{r^*}\right) - \ln\left(\frac{r_{k-1}}{r^*}\right)}}$$
$$+\, 2\sum_k \frac{a_k^d}{r_{k+1} - r_k}\left(\frac{\lambda_0}{\lambda}\right)^{\frac{b_k^d\ln\left(\frac{r_{k+1}}{r^*}\right) - b_{k+1}^d\ln\left(\frac{r_k}{r^*}\right)}{\ln\left(\frac{r_{k+1}}{r^*}\right) - \ln\left(\frac{r_k}{r^*}\right)}}\int_{r_k^*}^{r_{k+1}^*} dr\, \frac{r\,(r_{k+1} - r)}{\sqrt{r^2-r_0^2}}\left(\frac{r}{r^*}\right)^{\ln\left(\frac{\lambda_0}{\lambda}\right)\frac{-b_k^d + b_{k+1}^d}{\ln\left(\frac{r_{k+1}}{r^*}\right) - \ln\left(\frac{r_k}{r^*}\right)}} \quad (8)$$

with $r_k^* = \max(r_0, r_k)$ ($r^*$ is a reference radial distance used to adimentionalize the argument of the logarithm and keep the computation numerically manageable). All the integrals we need to compute therefore have the form

$$\mathcal{J}^d(p,n,r_0,R) = \int_{r_0}^{R} dr\, \frac{r}{\sqrt{r^2-r_0^2}}\, r^n\left(\frac{r}{r^*}\right)^p \quad (9)$$

Using the substitution x=r/r0 and then $y = \sqrt{x^2-1}$ we obtain

$$\mathcal{J}^d(p,n,r_0,R) = \left(\frac{r_0}{r^*}\right)^p r_0\int_0^{\sqrt{\left(\frac{R}{r_0}\right)^2-1}} dy\,(y^2+1)^{p/2} \quad (10)$$

Substituting again : $v = \frac{y}{\sqrt{\left(\frac{R}{r_0}\right)^2-1}}$ and then $t = v^2$ we finally get

$$\mathcal{J}^d(p,n,r_0,R) = \frac{1}{2}\left(\frac{r_0}{r^*}\right)^p r_0\sqrt{\left(\frac{R}{r_0}\right)^2-1}\int_0^1 dt\, t^{-\frac{1}{2}}\left(1 - \left(1 - \left(\frac{R}{r_0}\right)^2\right)t\right)^{p/2} \quad (11)$$

Apply now Euler's integral definition of Gauss's hypergeometric ${}_2F_1$ function:

$${}_2F_1(a,b,c,z) = \frac{\Gamma(c)}{\Gamma(b)\Gamma(c-b)}\int_0^1 dt\, t^{b-1}(1-t)^{c-b-1}(1-z\,t)^{-a} \quad \text{(Euler)}$$

$${}_2F_1(a,b,c,z) = \sum_{n=0}^{\infty}\frac{(a)_n\,(b)_n}{(c)_n}\frac{z^n}{n!} \quad \text{(Gauss's hypergeometric function)} \quad (12)$$

$$(a)_n = a\,(a+1)(a+2)\dots(a+n-1) = \frac{\Gamma(a+n)}{\Gamma(a)} \quad \text{(Pochhammer symbol)}$$

Letting $z = 1 - \left(\frac{R}{r_0}\right)^2$, $a = -\frac{n+p}{2}$, $b = \frac{1}{2}$ and $c = \frac{3}{2}$, we directly find

$$\mathcal{J}^d(p,n,r_0,R) = \frac{1}{2}\left(\frac{r_0}{r^*}\right)^p r_0\left[z\;{}_2F_1\left(-\frac{n+p}{2},\frac{1}{2},\frac{3}{2},-z^2\right)\right]_{z=\sqrt{\left(\frac{R}{r_0}\right)^2-1}} \quad (13)$$

and the dust optical thickness becomes

$$\tau_{dust} = 2\sum_k \frac{a_k^d}{r_k - r_{k-1}}\left(\frac{\lambda_0}{\lambda}\right)^{\frac{b_{k-1}^d\ln\left(\frac{r_k}{r^*}\right) - b_k^d\ln\left(\frac{r_{k-1}}{r^*}\right)}{\ln\left(\frac{r_k}{r^*}\right) - \ln\left(\frac{r_{k-1}}{r^*}\right)}}\Big[\mathcal{J}^d(p,1,r_0,r_k^*) - \mathcal{J}^d(p,1,r_0,r_{k-1}^*) - r_{k-1}\left(\mathcal{J}^d(p,0,r_0,r_k^*) - \mathcal{J}^d(p,0,r_0,r_{k-1}^*)\right)\Big]_{p=\ln\left(\frac{\lambda_0}{\lambda}\right)\frac{-b_{k-1}^d + b_k^d}{\ln\left(\frac{r_k}{r^*}\right) - \ln\left(\frac{r_{k-1}}{r^*}\right)}}$$
$$+\, 2\sum_k \frac{a_k^d}{r_{k+1} - r_k}\left(\frac{\lambda_0}{\lambda}\right)^{\frac{b_k^d\ln\left(\frac{r_{k+1}}{r^*}\right) - b_{k+1}^d\ln\left(\frac{r_k}{r^*}\right)}{\ln\left(\frac{r_{k+1}}{r^*}\right) - \ln\left(\frac{r_k}{r^*}\right)}}\Big[-\left(\mathcal{J}^d(p,1,r_0,r_{k+1}^*) - \mathcal{J}^d(p,1,r_0,r_k^*)\right) + r_{k+1}\left(\mathcal{J}^d(p,0,r_0,r_{k+1}^*) - \mathcal{J}^d(p,0,r_0,r_k^*)\right)\Big]_{p=\ln\left(\frac{\lambda_0}{\lambda}\right)\frac{-b_k^d + b_{k+1}^d}{\ln\left(\frac{r_{k+1}}{r^*}\right) - \ln\left(\frac{r_k}{r^*}\right)}} \quad (14)$$

Expressions (14), (13) and (12) can be used to compute the $K_k$ Abel transforms in (6), possibly using standard identities to stabilize the ${}_2F_1$ series when its arguments produce an alternating series . Expression (14) also implies differences of $\mathcal{J}^d$ integrals, which can be nearly equal numbers in real applications. One can then alternatively use equation (10) with an appropriate lower bound and use a Gauss-Legendre (G-L) integration method to efficiently avoid the numerically troublesome differences. G-L method of order n exactly integrates a polynomial of power up to 2n-1. The integrant of (10) being a simple (non-integer) power, one can expect a G-L method of sufficiently high order will produce machine-precision accurate results. We only focus here on the fitting of the linear parameters, but we already highlight that an iterative method aimed at determining the $b_k^d$ can be imagined, the derivative of $\mathcal{J}^d(p,n,r_0,R)$ with respect to p being easily obtained in series (12) an integral (10).

## Tests and applications to pseudo-data

We conducted tests aimed at assessing the properties of the inversion methods applied to artificially simulated signals, including a noise or not, using stepwise $u_k$ (the simplest choice mentioned in the preceding section) and then equations (7) to (14). We use a realistic $CO_2$ profile from Krasnopolski. The $O_3$ density is a Chapman profile with properties compatible with Lebonnois et al. [2006]. Our dust properties profile mimic one of those published by Matthanen et al. [2013], chosen for its challanging numerical properties (i.e. mixing locally large and small gradients). The absorption cross sections are from Shemansky for $CO_2$ and from Malicet [1995]. We use 100 wavelength bins over the [200, 300] nm interval and the solar spectral distribution is from the Solar2000 model. The resulting detailed exponential attenuation of the solar radiation at 300 nm is detailed below. The total attenuation is the product of those from the dusts, $CO_2$ and $O_3$. In our test, the dusts vastly dominate over the other contributions.

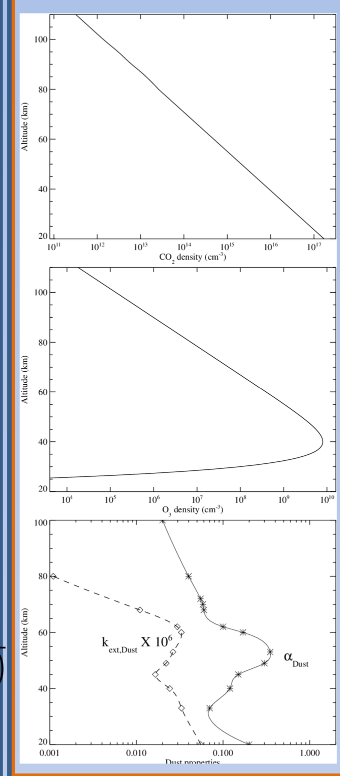


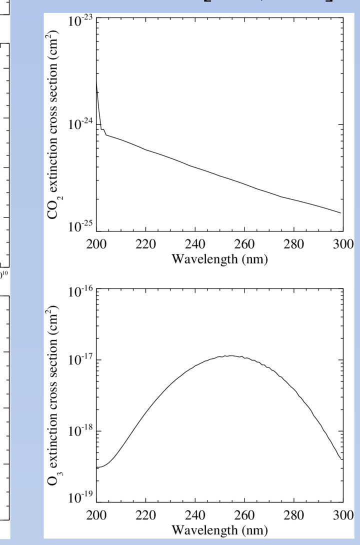


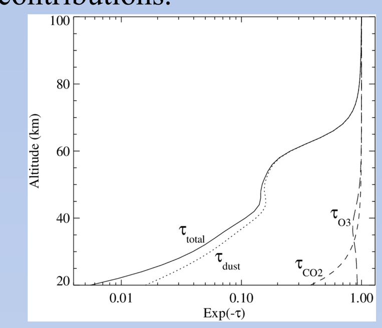


### Without noise

We compare the dust $k_{ext,0}$ profile as well as the $CO_2$ and $O_3$ density retrieved using stepwise and log-linear $u_k$ functions: Dashes represent the input profiles, dotted lines with stars show the retrieved value. The piecewise log-linear representation of the α(r) parameter brings a somewhat more accurate representation , which improves the retrieval of the less absorbing species. For the plots shown here, we used twice more pseudo-data points than fitting points. The benefit is more important when the number of data and fitting points are equal. It must be noted that a regularization of the system is necessary. We penalized the second derivative of the $a_k$'s.

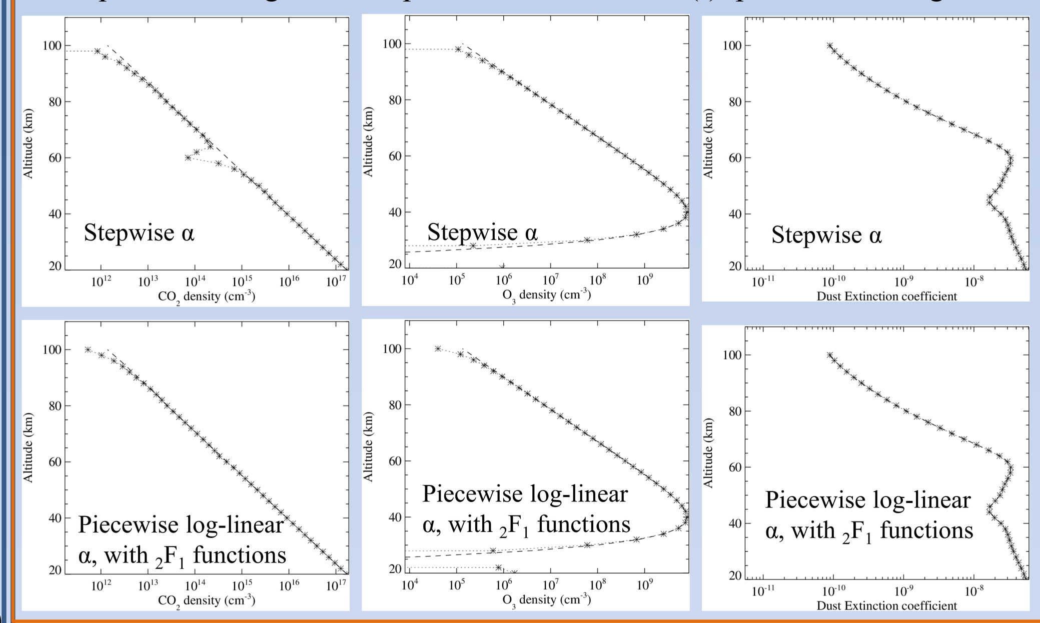


### With noise

Noise necessarily degrades the information provided by the (pseudo-)data. We included a minor noise to the simulated intensity, following a Poisson statistics. The relative uncertainty is small, as would be the case when using a high efficiency detector. Again, using the log-linear functions for the α(r) parameter improves the retrieval of $CO_2$. The adverse effect of noise can however easily impair the retrieval quality of the less absorbing species.

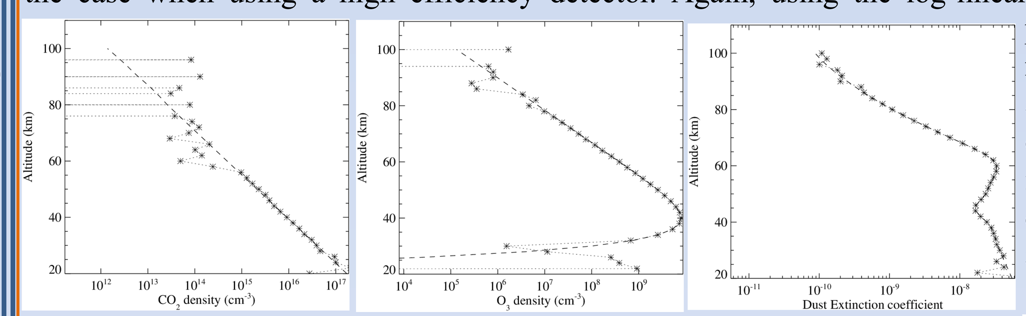


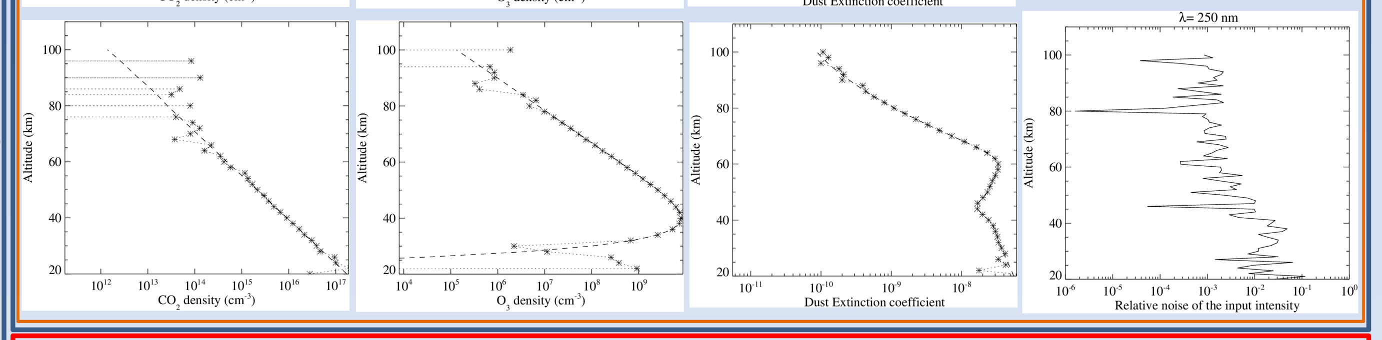


## Conclusions:

- Analytical expressions are found that allow for a log-linear piecewise, continuous representation of the vertical profile of the dust properties, for which the Abel transform of each piece can be computed using hypergeometric ${}_2F_1$ functions.
- Inclusion of the piece-wise linear triangular elements in the inverse Abel transform analysis of (simulated) occultation of the solar UV radiation by the Mars atmosphere allows for a more accurate retrieval of the $O_3$, $CO_2$ and dust extinction profiles, provided that a very sensitive detection is performed, the inversion being sensitive to noise.
- Further developments will be undertaken to fit the vertical profile of the dust extinction α(r) parameter, computation of the ${}_2F_1$ function being relatively fast.


References:

Hubert, B., C. Opitom , D. Hutsemekers , E. Jehin, G. Munhoven, J. Manfroid, D.V. Bisikalo, V.I. Shematovich, An inversion method for cometary atmospheres, Icarus, doi: 10.1016/j.icarus.2016.04.044, 2016.

Krasnopolski V.A., Mars' upper atmosphere and ionosphere at low, medium, and high solar activities: Implications for evolution of water, *J. Geophys. Res.*,107, doi:10.1029/2001JE001809, 2002.

Lebonnois S., Quémerais E., Montmessin F., Lefèvre F., Perrier S., Bertaux J.-L., and Forget F., Vertical distribution of ozone on Mars as measured by SPICAM/Mars Express using stellar occultations, *J. Geophys. Res.*, 111, 2006.

Määttänen A., Litowski C., Montmessin F., Maltagliati L., Reberac A., Joly L. and Bertaux J.-L., A complete climatology of the aerosol vertical distribution on Mars from Mex/SPICAM UV solar occultations, *Icarus*, 223, 892, 2013.

O'Niel N. and Royer A., Extraction of bimodal aerosol-size distribution radii from spectral and angular slope (Angstrom) coefficients, *Applied Optics*, 32, 1642, 1993.